Article:
Al-Sallami, W, Al-Damook, A and Thompson, HM (2017) A Numerical Investigation of the Thermal-Hydraulic Characteristics of Perforated Plate Fin Heat Sinks. International Journal of Thermal Sciences, 121. pp. 266-277. ISSN: 1290-0729

https://doi.org/10.1016/j.ijthermalsci.2017.07.022

A Numerical Investigation of the Thermal-Hydraulic Characteristics of Perforated Plate Fin Heat Sinks

Waleed Al-Sallami[1,*], Amer Al-Damook[1, 2], H.M. Thompson[1]

[1]School of Mechanical Engineering, University of Leeds, UK

[2]Mechanical Engineering Department, Faculty of Engineering, University of Anbar, Iraq.

Abstract

The benefits of using notch, slot and multiple circular perforations in plate fin heat sinks (PFHSs), are investigated numerically, using a conjugate heat transfer model. Comparisons show that each type of perforation can provide significantly reduced pressure drops over PFHSs but that fins with slot perforations provide the most effective design in terms of heat transfer and pressure drop. The practical benefits of each type of perforated fin for micro-electronics cooling is also explored and their capabilities of achieving low processor temperatures for reduced mechanical power consumption are quantified.

Keywords: perforated plate fins, k-ω SST model, conjugate heat transfer, electronic cooling applications.

NOMENCLATURE			
A_c	cross-sectional area of the flow passage of the heat sink, m^2	S	pin pitch in streamwise direction, mm
D	pin diameter of the pin fin heat sink, mm	Re	Reynolds number
d	perforation diameter of the pin fin, mm	T	temperature, ^oC
D_h	hydraulic diameter, m	ΔT	temperature difference, ^oC
H	pin fin height, mm	U	air velocity, m/s
h_p	Projected heat transfer coefficient, $W/m^2.^oC$	T_{base}	CPU temperature, ^oC
h	heat transfer coefficient, $W/m^2.^oC$	**Greek**	
k	turbulence kinetic energy, $Kg.m^2s^{-2}$	α	fluid thermal diffusivity (m^2/s)
n	number of perforations	α,β,β*	turbulence model constant
N	number of pins	μ	fluid viscosity (Pa·s)
L	heat sink length, mm	μ_t	turbulent eddy viscosity, Pa.s
Nu	Nusselt number	ρ	fluid density (kg/m^3)
P_{fan}	fan power, W	ν	kinematic viscosity, m^2/s
ΔP	pressure drop, Pa	$_{\nu t}$	turbulent kinematic viscosity, m^2/s
Pr	Prandtl number	σ_ε	k-ε turbulence model constant
Pr_t	turbulent Prandtl number	σ	turbulence model constant for the k-equation
Q	power applied on the base, W	ω	k-ω turbulence model constant
p	Perimeter, m		

1. Introduction

Thermal management is a key challenge for the semiconductor industry, since the inexorable rise in heat flux densities from micro-electronic components and devices presents formidable challenges in maintaining processor temperatures below critical values, in order to avoid a range of important failure modes, such as chip cracking and thermal oxidation of interconnect

surfaces [1]. Since the cooling of electronics accounts for around 0.5% of global electricity consumption [2] innovative cooling solutions are required which can deal with very high heat flux densities over localized hot spots, in excess of 100W/cm^2, whilst also minimizing energy consumption [3]. These challenges have stimulated a number of cooling innovations, including the use of highly conductive inserts to provide more efficient pathways to heat removal [4], and a number of promising liquid cooling methods. The latter include on-chip cooling, direct liquid jet impingement and dielectric liquid immersion, which removes heat by convection currents [5], and the use of nanofluids as a means of increasing convective heat transfer [6].

This paper focusses on what is currently the most popular approach for cooling microelectronics due to its low cost, availability and reliability, namely convective heat transfer to air as it flows over a network of extended surface fins on a heat sink [7]. The reader is referred to the recent seventy-paper review by Nagarini et al. [8] for a summary of the main innovations in the design of extended surface heat exchangers in the last two decades. These have demonstrated clearly that surface fins offer a practical means of achieving large heat transfer area, without excessive primary surface area, and act as turbulence promoters thus further enhancing heat transfer rates [9]. It has recently been estimated that heat sinks, fans and blowers account for more than 80% of the thermal management solutions for electronics, and that these will be worth over $14 billion by 2021 [10]. Heat sinks provide a low cost and reliable means of achieving a large total heat transfer surface area without excessive primary surface area and the surface fins act as turbulence promoters which enhance heat transfer rates by breaking up the thermal boundary layer. The main goals of heat sink design are to provide the required heat transfer rates, to ensure processor temperatures remain below critical values, for minimal pressure loss and heat sink mass [8].

A number of studies have considered the performance of heat sinks with pins fins, termed Pinned Heat Sinks (PHSs) [9]. Soodphakdee et al [11] and Jonsson and Moshfegh [12], for example, investigated the effect of pin cross-sectional shape whilst Zhou & Catton [7] and Yang & Peng [13,14] considered the benefits of combining plate and pin fins within compound heat sinks. More recently, attention has turned to the benefits of perforating the pins within PHSs. Sahin and Demir [15, 16] studied the effect of the cross-sectional shape of perforations (circular or square) for in-line pin arrays while Dhumne and Farkade [17] considered the effect of staggered pin arrangements for singly-perforated pins of circular cross-section. Dai et al [18] studied the benefits of using micro-jets to improve heat transfer rate and reduce pressure drop by inducing flow separation in PHSs.

Al-Damook et al [9] have very recently used complementary experimental and numerical methods to explore the benefits of using multiple circular perforations within PHSs with circular pins. They showed that the Nusselt number increases monotonically with the number of perforations, while pressure drop/mechanical power consumption reduce monotonically. These benefits were found to arise not only due to the increased surface area but also due to the formation of localized air jets. Al-Damook et al [19] extended this work to compare the performance of multiple circular, square and elliptic perforations in PHSs. They showed that the optimal design may be a compromise between elliptic perforations, which minimize pressure drop, and circular perforations which provide the most effective heat transfer. Similar benefits have recently been reported for PHSs with pins perforated by much simpler single rectangular notch or slot perforations, which can also offer substantially improved performance, compared to solid pins, with reduced manufacturing complexity [20].

In spite of the attractiveness of PHSs in a number of applications, heat sinks based on rectangular plate fins, termed Plate Fin Heat Sinks (PFHSs) remain by far the most common. This is due to a number of important practical advantages over PHSs including simple structure, ease of manufacturing and comparatively small pressure drops/mechanical power consumption. A number of studies have examined how heat transfer rates can be improved by limiting the regions where air flows smoothly through the heat sink channels. Chiang [21] and Kotcioglu et al. [22], for example, used experimental Taguchi methods to optimize PFHS design, with the latter examining how periodically interrupted diverging and converging fins can enhance heat transfer significantly due to boundary layer disturbances and secondary mxing. Najafi et al. [23] adopted a numerical approach, using multi-objective Genetic Algorithms to optimize plate fin geometries for total heat transfer rate and total annual costs while the recent review by Kumar Das and Ghosh [24] summarised the benefits of using multiple air streams in PFHSs.

They key importance of improving heat transfer rates from PFHSs has motivated a number of recent studies to explore whether heat transfer rates from PFHSs can be increased by perforating the fins either longitudinally, along the fins, or laterally, across them. Studies of longitudinal perforations include those of Shaeri & Yaghoubi [25,26], who used numerical methods to study thermal airflows through arrays of solid and longitudinally-perforated plate fins, where the latter are perforated with one or more rectangular perforations. They found perforations to be extremely beneficial: they reduced the size of the wakes behind the fins and the length of the recirculation zone around the lateral surface of the fins, while air jets through

the perforations increased the heat transfer rate. They also noted that these improvements can be realized with substantial reduction in weight, of up to 50%. Shaeri & Jen [27,28] also found substantial improvements using longitudinal perforations, with a single perforation increasing the heat transfer rate by up to 80%. Similar benefits have been reported recently for strip fin heat sinks, with fin aspect ratios between those of plate fins (large aspect ratio) and pin fins (aspect ratio≈1) [29].

Ismail [30] and Ismail et al [31] considered the effect of the shape of single and multiple longitudinal perforations and examined triangular, square, circular and hexagonal perforations. They found that circular, square and hexagonal longitudinal perforations all provide significant enhancements to heat transfer but that the pressure drop for circular perforations is significantly smaller than for the other perforation shapes. Ehtesum et al. [32] carried out an experimental investigation into the effect of the diameter and number of longitudinal circular perforations in PFHSs. Their results demonstrated that increasing the perforation diameter enhances heat transfer and reduces pressure drop significantly and that these benefits increased with an increasing number of perforations.

The effects of perforating plate fins for natural convection heat transfer has also been considered in a number of previous studies. Alessa and Al-Widyan [33], Alessa et al. [34] and Awarsarmol and Pise [35], for example, studied the effect of triangular, rectangular and circular perforations respectively. Awarsarmol and Pise [36] recently carried out an experimental study into the enhancement of natural convection of a perforated fin array with circular perforations of different diameter and angles of inclination, providing useful data for validating numerical methods for porous fins, see e.g. Kundu et al. [37].

The benefits of lateral plate fin perforations have also been considered. Dhanawade and Dhanawade [38] experimentally determined the effect of lateral circular perforations for plate fins on heat transfer. They found that perforations generally increase the Nusselt number and that the optimum perforation diameter is a function of applied heat flux density, with larger perforations being beneficial for low heat fluxes and smaller perforations better for higher heat flux densities. Yaghoubi et al [39,40] showed that lateral perforations in PFHSs are ineffective for laminar airflows but that they increase heat transfer for turbulent flows. Ismail et al [41] later studied the benefits of employing either lateral circular, square, triangular or hexagonal perforations for turbulent flow cases. They found that hexagonal perforations yielded the highest heat transfer rate, while triangular ones minimize the frictional drag.

The present study is motivated by the findings of a recent investigation into the use of notch and slot perforations in PHSs [20], which demonstrated that very simple and easy-to-manufacture notch perforations yielded significant performance enhancements, offering a much more practical alternative to internal fin perforations. This paper is the first to explore the benefits of using simple, longitudinal notch and slot perforations in PFHSs and to compare these against the performance of multiple longitudinal circular perforations. It is organized as follows. Section 2 describes the numerical conjugate heat transfer model for the thermal airflows over the PFHSs under consideration and the numerical methods used to solve them. Section 3 describes the validation of the numerical method and presents a comprehensive set of numerical solutions which explore the benefits of perforations for PFHSs. Conclusions are drawn in Section 4.

2. Numerical Method

2.1 Problem Description

The plate fin designs considered are shown in Fig. 1, and include both solid fins and those with circular, notch and slot perforations. Four fins with circular perforations of diameter 1mm are considered with one (1P), two (2P), three (3P) and four (4P) perforations. Three slotted fin designs with rectangular slot perforations of width 1mm and height 3 mm (RM3), 6 mm (RM6) and 10 mm (RM10) are also considered, as are three fin designs with rectangular notches removed from the top of the plate fin, each with a width of 1 mm and heights of 2.5 mm (RU2.5), 5 mm (RU5) and 7.5 mm (RU7.5). Notch perforations are by far the easiest to implement during manufacturing. The dimensions of the base plate, fin height and fin thickness are the same for all heat sinks and are equal to 50×50 mm, 10 mm and 2 mm, respectively. In all cases, eight fins are arranged on top of the base plate, as shown in Fig. 2. Following Al-Damook et al [9], the heat sinks are taken to be aluminium with thermal conductivity 202 W/m.K and a base plate thickness of 2 mm.

2.2 Conjugate Heat Transfer Model

Following Al-Damook et al [9], a conjugate heat transfer model for the turbulent airflow over the heat sinks is developed. The properties of air are based on the inlet temperature of 25°C and the inlet velocity ranges between 6.5 m/s and 12 m/s which leads to Reynolds numbers between 3500 and 6580, based on equations (1) and (2).

$$R_e = \rho U D_h / \mu \tag{1}$$

$$D_h = 4\frac{A_c}{p} \tag{2}$$

The airflow is considered to be steady, incompressible and turbulent, see e.g. [17-20], and the conjugate heat transfer model analyses the heat flux, which is transferred through the heat sink into the moving air through the coupled boundary condition shown in Fig. 3(a). The heat flux through the heat sink is computed by solving the conduction equation (3).

Zhou and Catton [7] modelled the turbulent air flow using a Reynolds-Averaged Navier-Stokes (RANS) form of the continuity, momentum and energy equations (4, 5 and 7) respectively.

$$\nabla.(k_s \nabla T_s) = 0 \tag{3}$$

$$\nabla.\underline{U} = 0 \tag{4}$$

$$\frac{\partial \underline{\underline{U}}}{\partial t} + \nabla.(\underline{\underline{U}}\,\underline{\underline{U}}) = \frac{1}{\rho}\nabla.\left(\underline{\underline{\sigma}} - \rho\overline{\underline{U}'}\,\overline{\underline{U}'}\right) \tag{5}$$

In equation (5) $\underline{\underline{\sigma}}$ is the Newtonian stress tensor which can be computed using equation (6)

$$\underline{\underline{\sigma}} = -p\underline{\underline{I}} + \mu\left(\nabla\underline{U} + [\nabla\underline{U}]^T\right) \text{and} -\rho\overline{\underline{U}'}\,\overline{\underline{U}'} = \mu_t\left(\nabla\underline{U} + [\nabla\underline{U}]^T\right) - 2/3(\rho k\underline{\underline{I}}) \tag{6}$$

where $\overline{\underline{U}'}$ and $\underline{U}$ are the fluctuation and average turbulent velocity vectors respectively, and p and $\underline{\underline{I}}$ represent the pressure and the unit tensor.

$$\frac{\partial T_f}{\partial t} + \underline{U}.\nabla T_f = \left(\frac{\nu}{\mathrm{Pr}} + \frac{\nu_t}{\mathrm{Pr}_t}\right)\nabla^2 T_f + \frac{Q}{\rho C_p} \tag{7}$$

Following a number of recent, successful models of thermal air flows over heat sinks, the k-ω SST model with automatic wall function treatment is used, see e.g. [7,9,20]. The governing equations of this model are given in equations (8-14):

$$\frac{\partial(\rho k)}{\partial t} + \nabla(\rho k\,\underline{U}) = \tilde{P}_k - \beta^*\rho k\omega + \nabla.\left[(\mu + \sigma_k\mu_t)\nabla k\right] \tag{8}$$

$$\frac{\partial(\rho\omega)}{\partial t} + \nabla(\rho\omega\,\underline{U}) = \alpha\rho S^2 - \beta\rho\omega^2 + \nabla.\left[(\mu + \sigma_\omega\mu_t)\nabla\omega\right] + 2(1-F_1)\rho\sigma_{\omega_2}\frac{1}{\omega}\nabla k.\nabla\omega \tag{9}$$

In equation (9) F_1 refers to blending function defined in equation (10), where $CD_{k\omega}$ and the turbulent eddy viscosity v_t are specified in equations (11) and (12) respectively. F_2 and S refer

to the second blending function and the invariant measure of the strain rate respectively and F_2 is calculated using equation (13).

$$F_1 = \tanh\left(\left\{\min\left[\max\left(\frac{\sqrt{k}}{\beta^* \omega y}, \frac{500\nu}{y^2\,\omega}\right), \frac{4\rho\sigma_{\omega_2} k}{C D_{k\omega} y^2}\right]\right\}^4\right) \tag{10}$$

$$C D_{k\omega} = \max\left(2\rho\sigma_{\omega_2}\frac{1}{\omega}\nabla k.\nabla\omega, 10^{-10}\right) \tag{11}$$

$$\nu_t = \frac{a_1 k}{\max(a_1\,\omega, S\,F_2)} \tag{12}$$

$$F_2 = \tanh\left(\left[\max\left\{2\frac{\sqrt{k}}{\beta^*\,\omega\,y}, \frac{500\nu}{y^2\,\omega}\right\}\right]^2\right) \tag{13}$$

Equation (14) is employed to limit the growth of flow stagnation regions.

$$P_k = \mu_t \frac{\partial u_i}{\partial x_j}\left(\frac{\partial u_i}{\partial x_j} + \frac{\partial u_j}{\partial x_i}\right) \rightarrow \tilde{P}_k = \min\left(P_k, 10\beta^*\,\rho\,k\,\omega\right) \tag{14}$$

The constants for the SST model are taken as:

$$\beta^* = 0.09, \alpha_1 = \frac{5}{9}, \beta_1 = \frac{3}{40}, \sigma_{k1} = 0.85, \sigma_{\omega_1} = 0.5, \alpha_2 = 0.44, \beta_2 = 0.0828, \sigma_{k2} = 1, \sigma_{\omega 2} = 0.856.$$

2.3 Boundary Conditions

Due to symmetry, the flow through only one row of fins is analysed [25], see Fig. 3(b). Following Al-Damook et al [9], the boundary conditions are given by:

1- On the bottom of the heat sink a uniform heat flux of 20000 W/m^2 and a no-slip condition, $U = 0$ are applied.
2- The inlet air temperature is 25^{o}C and its velocity ranges between 6.5 and 12 m/s.
3- At the outlet, the pressure and the temperature gradient are both set to zero ($\frac{dT}{dx} = 0$).
4- At the fin surfaces no slip, $U = 0$, and heat flux is conserved ($k_f.\frac{dTf}{dn} = k_s\frac{dT_s}{dn}$).
5- The left and right sides are taken to be symmetry boundaries.
6- All other walls, no slip and adiabatic conditions are applied.

Following a number of previous studies, e.g. [9], which have shown radiative heat transfer is small for the conditions considered here, radiative losses are neglected.

3. Results and Discussion

A commercial finite volume method (FVM)-based code, ANSYS FLUENT [42] is used to solve the fully coupled momentum and energy equations, using second order upwinding, while continuity is satisfied using the SIMPLE method in which the velocity components are first calculated from the Navier–Stokes equations using a guessed pressure field. Computation is started first by solving the continuity, momentum, k and ω equations to determine the flow field and then the energy equation to find the temperature field in the computational region. The procedure continues until the sum of the residuals of the continuity and momentum equations in each cell is less than 10^{-4} and the residuals of the energy equations are smaller than 10^{-6}.

3.1 Grid Independence and Validation Tests

The grid is composed of dense tetrahedral mesh elements to improve the quality of the numerical prediction near plate fin surfaces. The impact of grid density on the numerical solutions is investigated for the all examined models and the results for solid (0P) and slotted plate fins (RM10) are presented in Table 1. For the RM10 fins, increasing the number of cells above 799835 leads to a less than 0.5% variation in the base temperature and pressure drop. For solid fins, far fewer cells are needed and the results imply that grid independence is achieved with only 103449 cells.

The numerical approach adopted here is next validated for the cases of plate fins with longitudinal, circular perforations, against the numerical predictions of Ismail [30] and the experimental data of Ehteshum et al [32]. Figs. 4(a) and (b) compare the Nusselt number (Nu) and total drag predicted in the present study with the numerical results of Ismail [30]. The agreement is generally very good, and the average discrepancies for Nu and total drag are only 4% and 6% respectively. Fig. 4(c) and (d) compare the predictions of Nusselt number and pressure drop obtained here with the experimental data of Ehteshum et al [32]; once again, agreement is good and in this case the average discrepancies are only 3% and 7% for the Nusselt number and pressure drop respectively.

3.2 Effect of Fin Design on Fan Power Consumption

Fig. 5 demonstrates the effect of plate fin design on the fan power, P_{fan}, needed to overcome the pressure drop, calculated using equation (15), as the air flows through the heat sinks.

$$P_{fan} = U.A_{pf}.\Delta P \tag{15}$$

where U, A_{pf} and ΔP are the inlet air velocity, flow cross-sectional area A_{pf} = *H.S. (N-1)* and pressure drop over the heat sink respectively.

Fig 5(a) compares the fan power consumption for flow over PFHSs with solid and circularly-perforated fins. It shows that, for a given inlet air speed, the fan power decreases as the number of perforations increases and the average reduction percentages in comparison with solid fin are approximately 5%, 9%, 12% and 13% for the 1P, 2P, 3P and 4P fins respectively. Note that the benefits of increasing from three to four perforations are very small, suggesting that the extra manufacturing complexity with four perforations is not justified for these fin designs.

Fig.5 (b) shows that the fan power consumption for the notched fins reduces monotonically with notch height due to the increasing cross-sectional flow area. The average reduction percentages compared to the case with solid fins are approximately 5%, 14% and 20% for the RU2.5, RU5 and RU7.5 fins respectively. Fig.5 (c) considers the slotted fins and once again the fan power decreases as the slot height increases, with reductions of roughly 12%, 19% and 24% for the RM3, RM6 and RM10 fins respectively.

3.3 Effect of Fin Design on Heat Transfer Coefficient

The heat transfer coefficient of a heat sink depends on the choice of characteristic area used. Al-Damook et al [9] have recently shown that using the projected area heat transfer coefficient, h_P based on the projected cross-sectional area of the heat sink that is calculated using equation 16 is perhaps the most useful indicator of the heat transfer efficiency for practical considerations, where $A_p = WL$ the projected base area, L and W are length and width of heat sink respectively.

$$h_P = \frac{\dot{Q}}{A_p[T_w - (\frac{T_{out} + T_{in}}{2})]} \tag{16}$$

Fig. 6 shows the values of h_P for all fin designs and shows clearly that these are lowest for the solid fins, which is expected since these have has the smallest wetted area and have no localized jets due to the absence of perforations. Conversely, the RM10 fin has the largest wetted area in contact with the air and the largest value of h_P. Fig. 6(a) considers the circularly-perforated fins. Their values of h_P increase monotonically with the number of perforations, the average enhancements over solid fins being approximately 2%, 3%, 7% and 9% for the 1P, 2P, 3P and 4P fins respectively. The results also show how the benefits of the perforations increase significantly for the higher air speeds. Results for the notched fins are shown in Fig. 6(b). These show that the notches are more effective than circular perforated fins due to the higher wetted areas however the removal of material from the top of the fin rather than the bottom of the fin,

which conducts heat away from the heat sink may also be influential. The average enhancements over solid fins are 12%, 22% and 31% for the RU2.5, RU5 and RU 7.5 fins respectively.

Fig. 6(c) shows the heat transfer performance of the slotted fins. As expected, the highest heat transfer coefficient is for the RM10 model because the number of fins has in effect been doubled from 8 to 16 fins with thinner fin thicknesses. However, the heat transfer coefficients for slotted fins are similar to comparable to those obtained with the notched fins, in spite of their large wetted area. This may be due to the fact that removing metal near the heat sink, is compromising its ability to conduct heat away from the heat sink. The average enhancements compared to the solid fins for the notched fins are 12%, 22% and 35% for the RM3, RM6 and RM10 fins respectively.

3.4 Effect of Fin Design on CPU Temperature

The primary purpose of the heat sink in electronic systems is to ensure that the processor temperatures remain below critical temperatures to avoid component damage and failure. For PCs, for example, Yuan et al. [43] stated that this critical temperature is around 85^{o}C. This cooling should be achieved with minimal fan power consumption. The effect of fin design on the compromise between the average heat sink base temperature, T_{case}, and fan power is shown in Fig. 7. Fig 7(a) shows that when the fan power is less than roughly 0.06 W the circularly-perforated fins have a larger T_{case} whereas for fan powers greater than about 0.06W the solid fins have the hottest base temperature, in agreement with Ismail [30]. The average reductions in T_{case} compared to the solid fins are roughly 1%, 1%, 4% and 4% for the 1P, 2P, 3P and 4P fins respectively. For the notched fins, Fig. 7(b) shows that the heat sink base temperature is significantly lower in all cases with average reductions of 5%, 10% and 13% for the RU2.5, RU5 and RU7.5 fins respectively. For the slotted fins, Fig. 7(c) shows even greater reductions in T_{case} with average reductions of 6%, 11% and 16% for the RM3, RM6 and RM10 fins respectively, compared with those for the solid fins.

The temperature distribution on the fin surfaces with an air inlet velocity of 12m/s for the solid, 4P, RU7.5 and RM10 fins are shown in Fig. 8. As expected, the coolest fin surface is for the RM10 fin, whereas the hottest is clearly for the solid, 0P, fin.

3.5 Effect of Fin Design on Heat Sink Mass

Heat sinks for electronics cooling need to be as light as possible, while meeting their functional requirements on heat transfer and pressure drop, in order to reduce material consumption and

cost and to increase portability. The total mass of the heat sinks considered here has been calculated utilizing equations 17 and 18 and the values are showed in Table 2, where the density of aluminum $\rho_{Al} = 2712$ kg/m^3.

$$V_t = V_{base} + V_{fins} \tag{17}$$

$$m_t = \rho_{Al} \times V_t \tag{18}$$

Table 2 shows that using circularly-perforated, notched and slotted fins on heat sinks offer the additional advantage of a significant reduction in its mass, which for slotted fins is over 30%.

3.6 Effect of Fin Design on the Flow Field

Fig. 9 demonstrates the effect of the perforations in the 4P and RM10 models on the flow field in comparison with the flow field for the solid fin, 0P. Since the top views of the flow field for the slotted and notched fins are very similar, only the slotted fin case has been shown. These show that the perforations lead to a substantial reduction in the size of the recirculation region behind the fin, which acts to reduce the overall pressure drop. The enhancement in the rate of heat transfer is due to the combination of the increase in the wetted area in contact with the air and the creation of localized jets that lead to higher convective heat transfer, see also [20].

3.7 Overall Performance of Fin Designs

Table 3 summaries the performance benefits offered by the circular, notch and slot perforations for PFHSs in terms of h_p, ΔP and T_{case}, compared to heat sinks with solid plate fins. It shows that PFHSs with either RM10 or RU7.5 fins can provide efficient cooling of the heat sink base with minimal fan power consumption. Since notch perforations are the easiest to manufacture, the slightly better performance of the slot perforations may not be worth the additional manufacturing complexity and costs associated with creating internal fin perforations.

4. Conclusions

Heat sinks with plate fins provide critical cooling in a range of important industries and practical applications and are particularly important in the electronics industry. Although several previous studies have explored the benefits of employing internal perforations in plate fins, the present study is the first to explore the benefits of using simple longitudinal notch and slot perforations in PFHSs and the first to compare their performance with multiple circular longitudinal perforations.

Results have shown that both notch and slot perforations offer significant advantages over circular perforations in terms of heat transfer and pressure drop and can achieve substantial

reductions in the heat sink base temperature, the fan power required to cool the base below critical temperatures and heat sink material volume and mass. Notched fins are relatively simple to manufacture [20] and may offer the most attractive design option since the marginal improvements offered by the slot perforations may not be worth the extra manufacturing complexity and costs.

Collectively, the results presented here have demonstrated that the design of perforated PFHSs offers a very interesting multi-objective design optimisation problem where an appropriate balance must be struck between maximizing heat transfer, whilst at the same time minimizing pressure drop/mechanical power consumption and heat sink mass. If manufacturing complexity is also considered, then notch perforations may well offer an attractive, effective and practical solution to the important problem of improving the performance of PFHSs. These compromises are currently being investigated in a formal optimisation study.

5. Acknowledgements

The authors would like to thank the Higher Committee for Education Development in Iraq (HCED), Iraqi Ministry of Higher Education and Scientific Research (MOHE), and Mechanical Engineering Department University of Anbar, Iraq for financial support of this work.

References

[1] S. Gurrum, S. Suman, Y. Joshi and A. Fedorov, "Thermal Issues in Next-Generation Integrated Circuits", *IEEE Transactions on Device and Materials Reliability*, vol. 4, no. 4, pp. 709-714, 2004.

[2]C.S. Sharma, M.K. Tiwari, S. Zimmerman, T. Brunschwiler, G. Schlottig, B. Michel, D. Poulikakos, “Energy efficient hotspot-targeted embedded liquid cooling of electronics”, *Applied Energy*, vol. 138, pp 414-422, 2015.

[3]International Technology Roadmap for Semiconductors 2.0, Heterogeneous Integration, 2015. [Online]. Available: https://www.dropbox.com/sh/3jfh5fq634b5yqu/AADYT8V2Nj5bX6C5q764kUg4a?dl=0. [Accessed: 30-May-2017].

[4] M. Hajmohammadi, V. Alizadeh Abianeh, M. Moezzinajafabadi and M. Daneshi, "Fork-shaped highly conductive pathways for maximum cooling in a heat generating piece", *Applied Thermal Engineering*, vol. 61, no. 2, pp. 228-235, 2013.

[5] P. Hopton and J. Summers, "Enclosed liquid natural convection as a means of transferring heat from microelectronics to cold plates", *Semiconductor Thermal Measurement and Management Symposium (SEMI-THERM), 2013 29th Annual IEEE*, pp. 60 - 64, 2013.

[6] A. Ijam and R. Saidur, "Nanofluid as a coolant for electronic devices (cooling of electronic devices)", *Applied Thermal Engineering*, vol. 32, pp. 76-82, 2012.

[7] F. Zhou and I. Catton, "Numerical Evaluation of Flow and Heat Transfer in Plate-Pin Fin Heat Sinks with Various Pin Cross-Sections", *Numerical Heat Transfer, Part A: Applications*, vol. 60, no. 2, pp. 107-128, 2011.

[8] N. Nagarani, K. Mayilsamy, A. Murugesan and G. Kumar, "Review of utilization of extended surfaces in heat transfer problems", *Renewable and Sustainable Energy Reviews*, vol. 29, pp. 604-613, 2014.

[9] A. Al-Damook, N. Kapur, J. Summers and H. Thompson, 'An experimental and computational investigation of thermal air flows through perforated pin heat sinks', *Applied Thermal Engineering*, vol. 89, pp. 365-376, 2015.

[10] A. McWilliams, "The Market for Thermal Management Technologies - SMC024G", *Bccresearch.com*, 2015. [Online]. Available: http://www.bccresearch.com/market-research/semiconductor-manufacturing/thermal-management-technologies-market-smc024g.html. [Accessed: 22- Dec- 2015].

[11]D. Soodphakdee, M. Behnia, D.W. Copeland, “A comparison of fin geometries for heat sinks in laminar forced convection Part 1: round elliptical, and plate fins in staggered and in-line configurations”, *Int. J. Microcircuits Electron. Packag*., vol. 24, pp 68-76, 2001.

[12] H. Jonsson, B. Moshfegh, “Modelling of the thermal and hydraulic performance of plate fin, strip, fin, and pin fin heat sinks-influence of flow bypass”, *Components Packag. Technol. IEEE Trans.*, vol. 24, pp 142-149, 2001.

[13]Y.T. Yang and H.S. Peng, “Investigation of planted pin fins for heat transfer enhancement in plate fin heat sink”, *Microelectron. Reliab.,* vol. 49, pp 163-169, 2009.

[14]Y.T. Yang and H.S. Peng, “Numerical study of thermal and hydraulic performance of compound heat sink”, *Numer. Heat Transf. Part A: Appl*., vol. 55, pp 432-447, 2009.

[15] B. Sahin and A. Demir, “Thermal performance analysis and optimum design parameters of heat exchanger having perforated pin fins”, *Energy Conversion and Management*, vol. 49,

no. 6, pp. 1684-1695, 2008.

[16] B. Sahin and A. Demir, “Performance analysis of a heat exchanger having perforated square fins”, *Applied Thermal Engineering*, vol. 28, no. 5-6, pp. 621-632, 2008.

[17] A. Dhumne and H. Farkade, 'Heat transfer analysis of cylindrical perforated fins in staggered arrangement', *International Journal of Engineering Science and Technology (IJEST)*, vol. 6, pp. 125-138, 2013.

[18] X. Dai, F. Yang, R. Fang, T. Yemame, J. Khan and C. Li, "Enhanced single- and two-phase transport phenomena using flow separation in a microgap with copper woven mesh coatings", *Applied Thermal Engineering*, vol. 54, no. 1, pp. 281-288, 2013.

[19] Al-Damook, J. Summers, N. Kapur and H. Thompson, "Effect of Different Perforations Shapes on the Thermal-hydraulic Performance of Perforated Pinned Heat Sinks", *Journal of Multidisciplinary Engineering Science and Technology*, vol. 3, p. 4, 2016.

[20] A. Al-Damook, N. Kapur, J. Summers and H. Thompson, "Computational design and optimization of pin fin heat sinks with rectangular perforations", *Applied Thermal Engineering*, vol. 105, pp 691-703,2016.

[21] K. Chiang, "Optimization of the design parameters of Parallel-Plain Fin heat sink module cooling phenomenon based on the Taguchi method", *International Communications in Heat and Mass Transfer*, vol. 32, no. 9, pp. 1193-1201, 2005.

[22] I. Kotcioglu, A. Cansiz, M. Nasiri Khalaji, ‘Experimental investigation for optimization of design parameters in a rectangular duct with plate-fins heat exchanger by Taguchi method’, *Applied Thermal Engineering*, vol. 50, pp 604-613, 2013.

[23] H. Najafi, B. Najafi and P. Hoseinpoori, "Energy and cost optimization of a plate and fin heat exchanger using genetic algorithm", *Applied Thermal Engineering*, vol. 31, no. 10, pp. 1839-1847, 2011.

[24] P. Kumar Das, I. Ghosh, ‘Thermal design of multistream plate fin heat exchangers – a state-of-the-art review’, *Heat Transf. Eng*., vol. 33(4-5), pp 284-300, 2012.

[25] M.R. Shaeri and M. Yaghoubi, "Numerical analysis of turbulent convection heat transfer from an array of perforated fins", *International Journal of Heat and Fluid Flow*, vol. 30, no. 2, pp. 218-228, 2009.

[26] M.R. Shaeri and M. Yaghoubi, 'Thermal enhancement from heat sinks by using perforated fins', *Energy Convers. Manag*., vol. 50(5), pp 1264-1270, 2009.

[27] M.R. Shaeri and T.C. Jen, 'The effects of perforation sizes on laminar heat transfer characteristics of an array of perforated fins', *Energy Convers. Manag*. Vol. 64, pp 328-334, 2012.

[28] M.R. Shaeri and T.C. Jen, 'Turbulent heat transfer analysis of a three-dimensional array of perforated fins due to changes in perforation sizes', *Numer. Heat Transf. Part A: Appl*., vol. 61(11), p 16, 2012.

[29] W. Al-Sallami, A. Al-Damook and H. Thompson, "A numerical investigation of thermal airflows over strip fin heat sinks", *International Communications in Heat and Mass Transfer*, vol. 75, pp. 183-191, 2016.

[30] M. Ismail, "Effects of Perforations on the Thermal and Fluid Dynamic Performance of a Heat Exchanger", *IEEE Transactions on Components, Packaging and Manufacturing Technology*, vol. 3, no. 7, pp. 1178-1185, 2013.

[31] M.F. Ismail, M.O. Reza, M.A. Zobaer, M. Ali, 'Numerical investigation of turbulent heat convection from solid and longitudinally perforated rectangular fins', *Procedia Engineering*, 56, 497-454, 2013.

[32]M. Ehteshum, M. Ali, M. Islam and M. Tabassum, "Thermal and Hydraulic Performance Analysis of Rectangular Fin Arrays with Perforation Size and Number", *Procedia Engineering*, vol. 105, pp. 184-191, 2015.

[33] A. H. Alessa, M.I. Al-Widyan, 'Enhancement of natural convection heat transfer from a fin by rectangular perforations of bases parallel and toward its tip', *Appl. Math. Mech.-Engl. Ed.* 29(8), 2008, 1033-1044.

[34] A.H. Alessa, A.M. Maqableh, S. Ammourah, 'Enhancement of natural convection heat transfer from a fin by rectangular perforations with aspect ratio of two', *Int. J. Phy. Sci.,* 4(10), 540-547, 2009.

[35] U.V. Awarsarmol, A.T. Pise, 'Investigation of enhancement of natural convection heat transfer from engine cylinder with permeable fins', *Int. J. Mech. Eng. Technol*. 1, 238-247, 2010.

[36]U. Awasarmol and A. Pise, "An experimental investigation of natural convection heat transfer enhancement from perforated rectangular fins array at different inclinations", *Experimental Thermal and Fluid Science,* vol. 68, pp. 145-154, 2015

[37]B. Kundu, D. Bhanja, K-S Lee, 'A model on the basis of analytics for computing maximum heat transfer in porous fins', *Int. J. Heat Mass Transfer*, 55 (25-26), 7611-7622, 2012.

[38] K. H. Dhanawade and H. S. Dhanawade, "Enhancement of Forced Convection Heat Transfer from Fin Arrays with Circular Perforation". *IEEE, Frontiers in Automobile and Mechanical Engineering (FAME),* pp. 192-196, 2010.

[39] M. Yaghoubi, M.R. Shaeri, K. Jafapur, 'Three-dimensional numerical laminar convection heat transfer around lateral perforated fins', *Computational Thermal Sciences: An International Journal*, vol. 1(3), pp 323-340, 2009.

[40] M. Yaghoubi, M.R. Shaeri, K. Jafarpur, 'Heat transfer analysis of lateral perforated fin heat sinks', *Applied Energy*, vol. 86(10), pp 2019-2029, 2009.

[41] M.F. Ismail, M.N. Hasan, S.C. Saha, 'Numerical study of turbulent fluid flow and heat transfer in lateral perforated extended surfaces', *Energy*, vol. 64, pp 632-639, 2014.

[42] A. Fluent, 12.0 Theory Guide. Ansys Inc, 2009.

[43] W. Yuan, J. Zhao, C. Tso, T. Wu, W. Liu and T. Ming, "Numerical simulation of the thermal hydraulic performance of a plate pin fin heat sink", Applied Thermal Engineering, vol. 48, pp. 81-88, 2012.

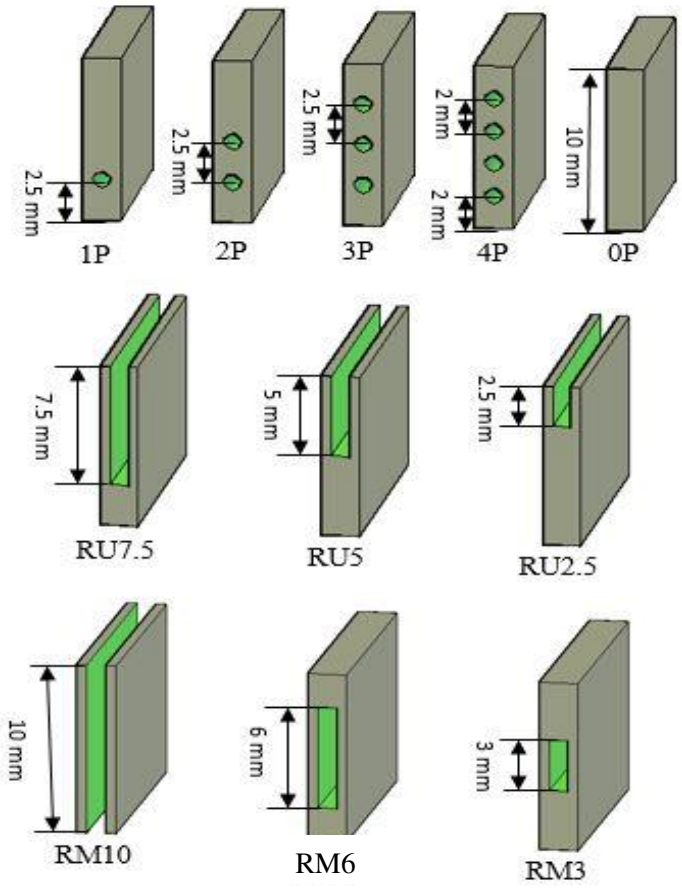

Fig.1: The eleven perforated plate fin designs considered

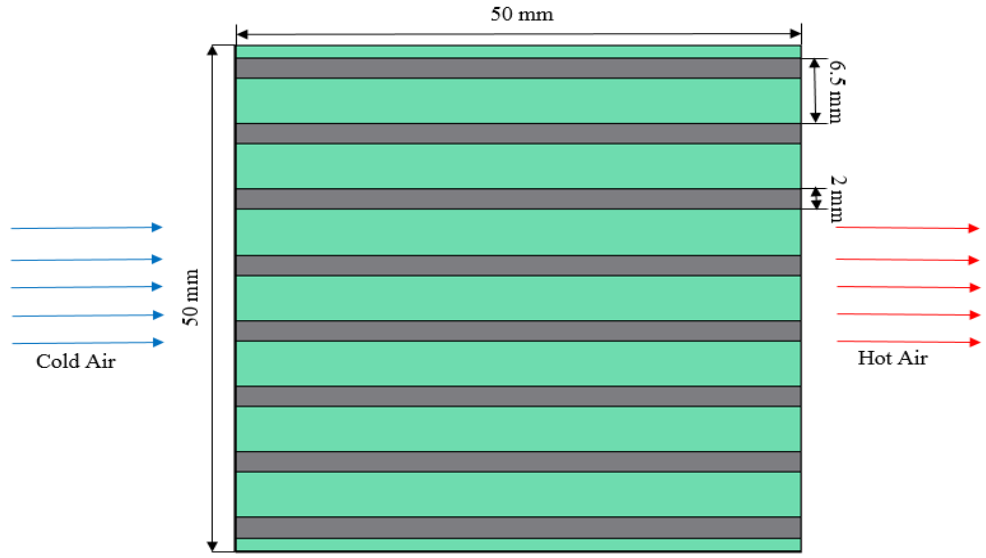

Fig. 2: Schematic diagram of examined plate fin heat sink.

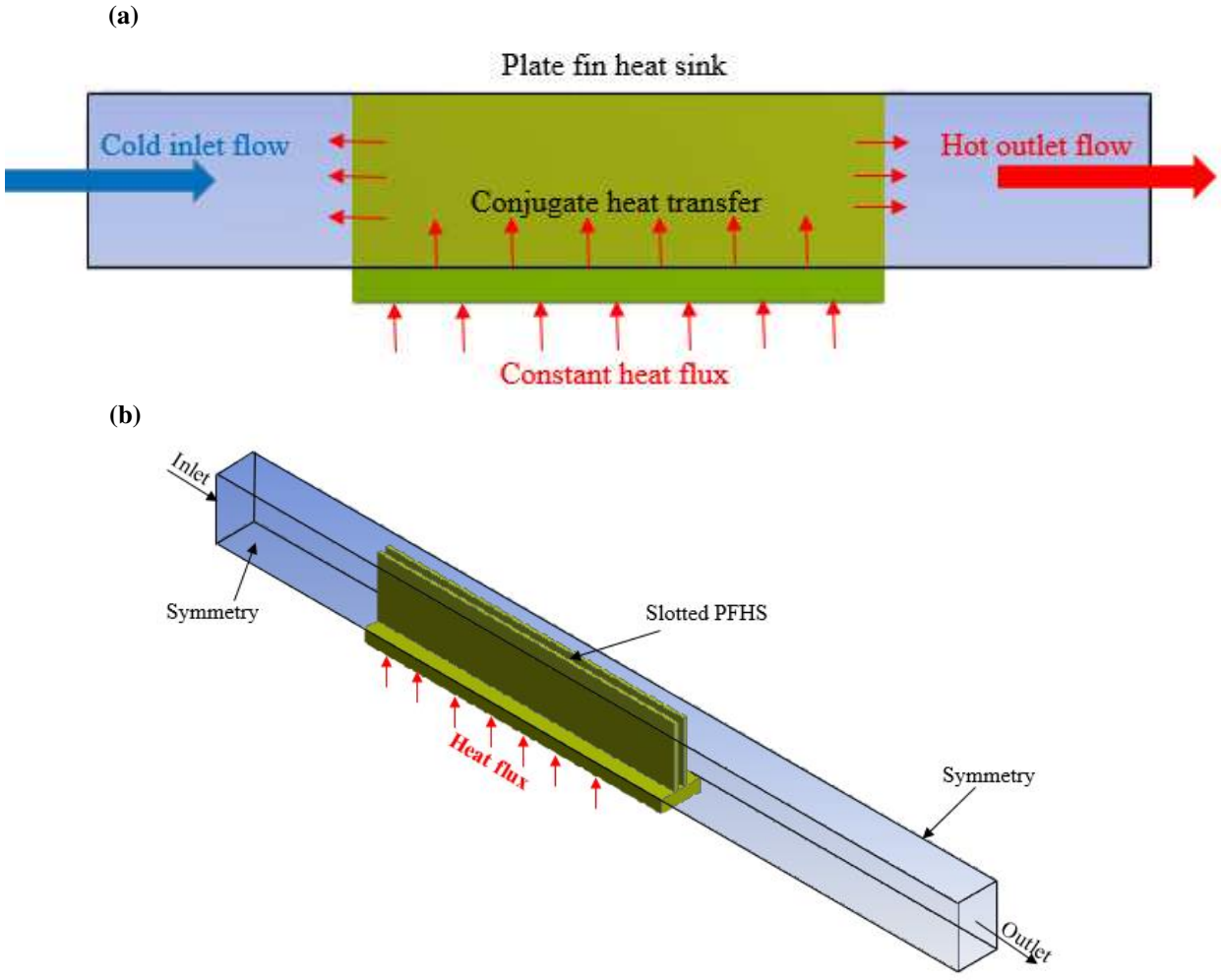

Fig. 3: (a) Conjugate heat transfer process; (b) the computational domain.

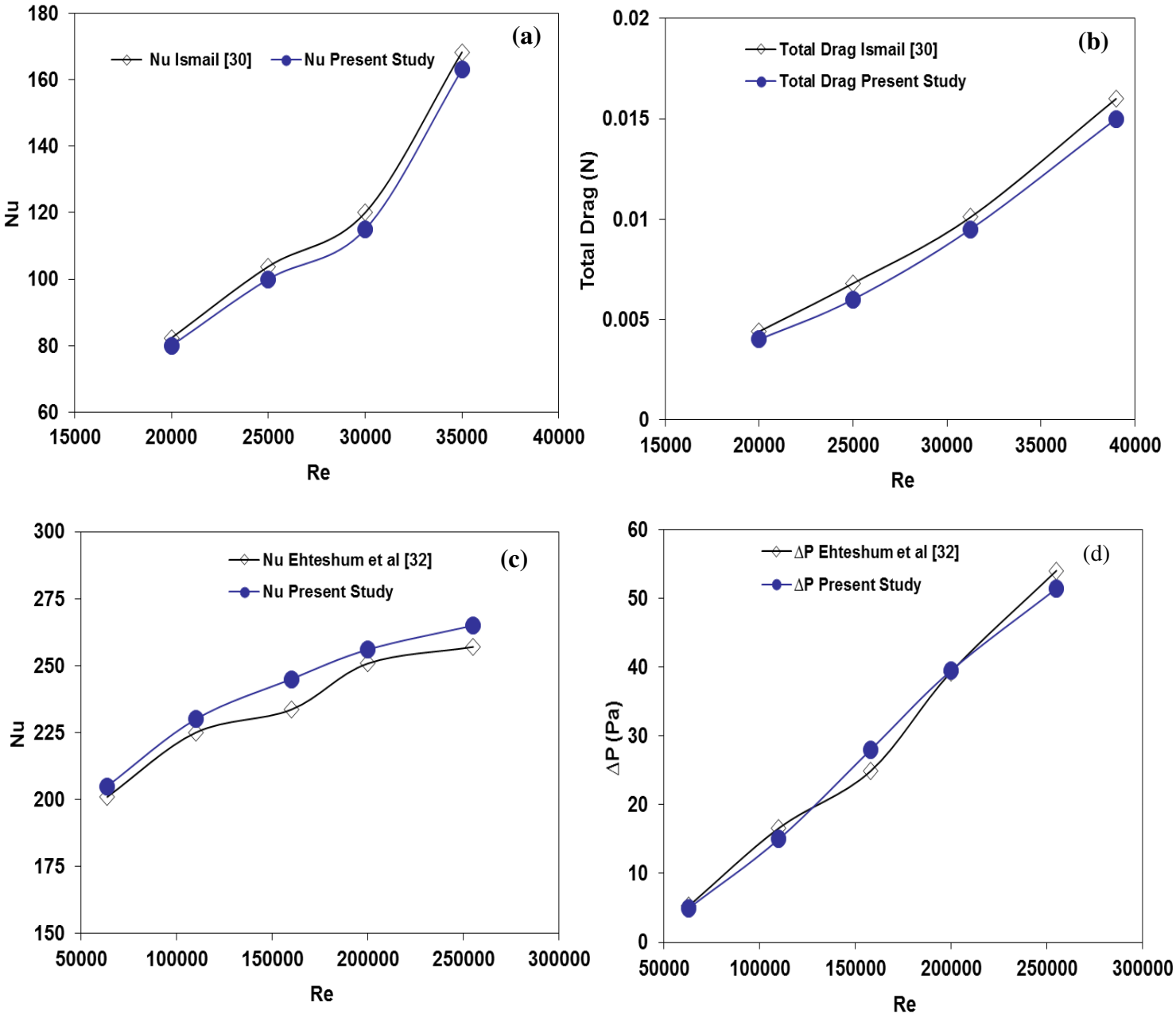

Fig. 4: Comparison between predictions for PFHSs with longitudinal, circular perforations against (a) Nu predicted numerical by Ismail [30]; (b) Total drag predicted by Ismail [30]; (c) Nu measured experimentally by Ehteshum et al [32]; (d) pressure drop measured experimentally by Ehteshum et al [32].

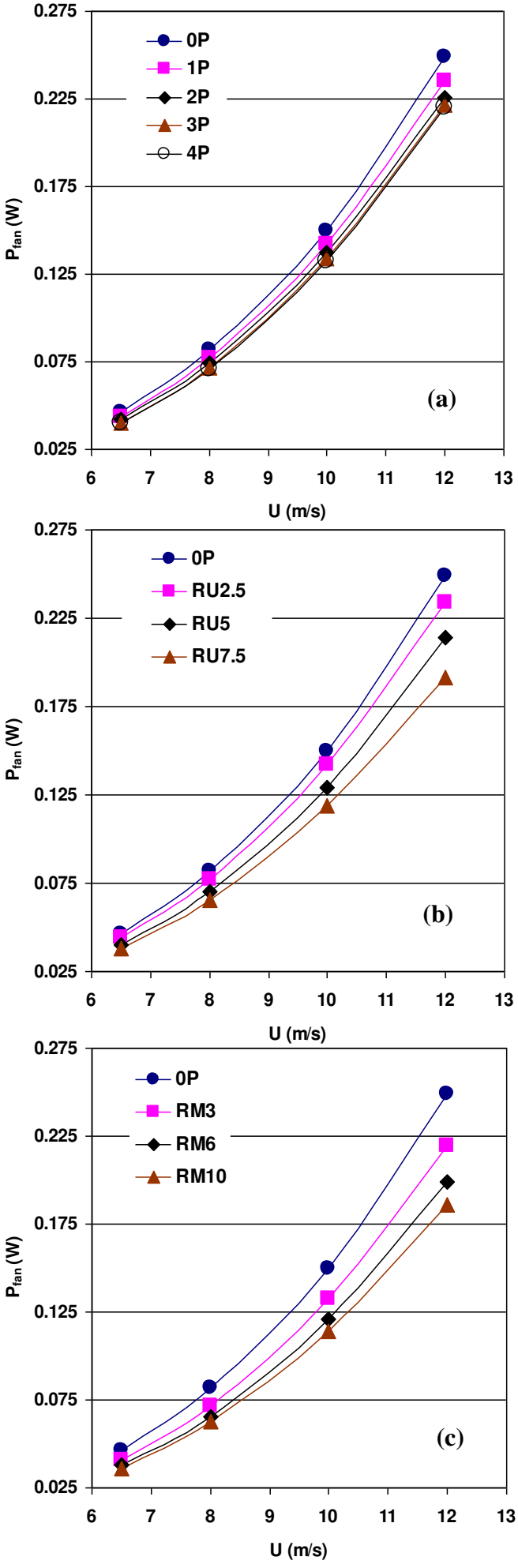

Fig. 5: Fan power for (a) solid and circular-perforated fins;

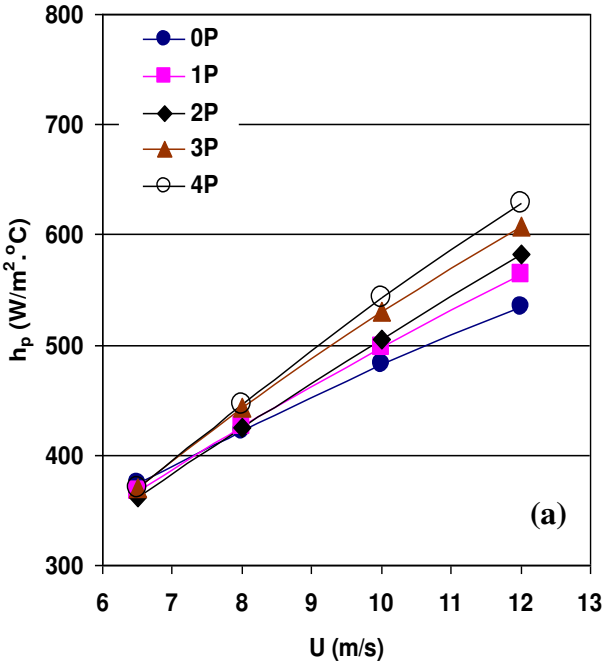
800
700
600
500
400
300
6
7
8
9
10
11
12
13
0P
1P
2P
3P
4P
h_p (W/m^2.°C)
U (m/s)
(a)

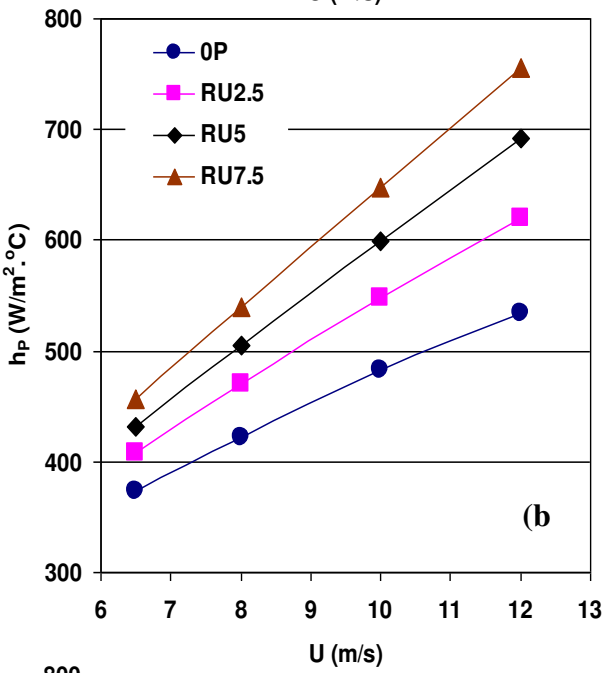
800
700
600
500
400
300
6
7
8
9
10
11
12
13
0P
RU2.5
RU5
RU7.5
h_P (W/m^2.°C)
U (m/s)
(b

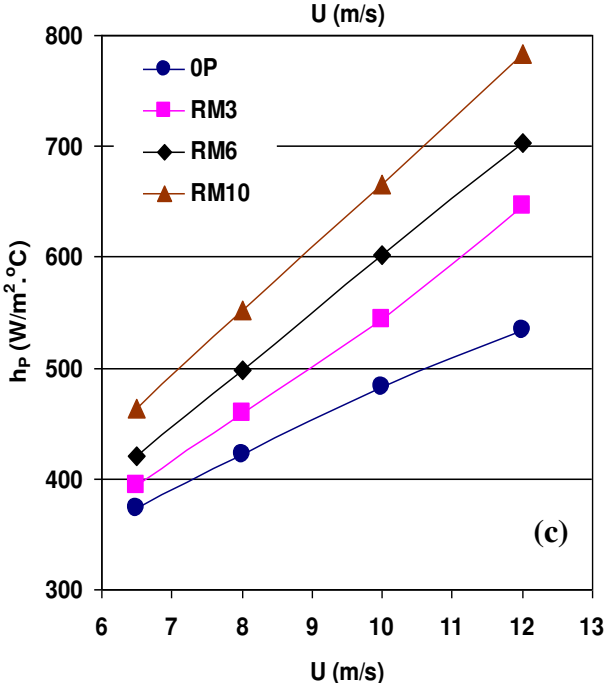
800
700
600
500
400
300
6
7
8
9
10
11
12
13
0P
RM3
RM6
RM10
h_P (W/m^2.°C)
U (m/s)
(c)

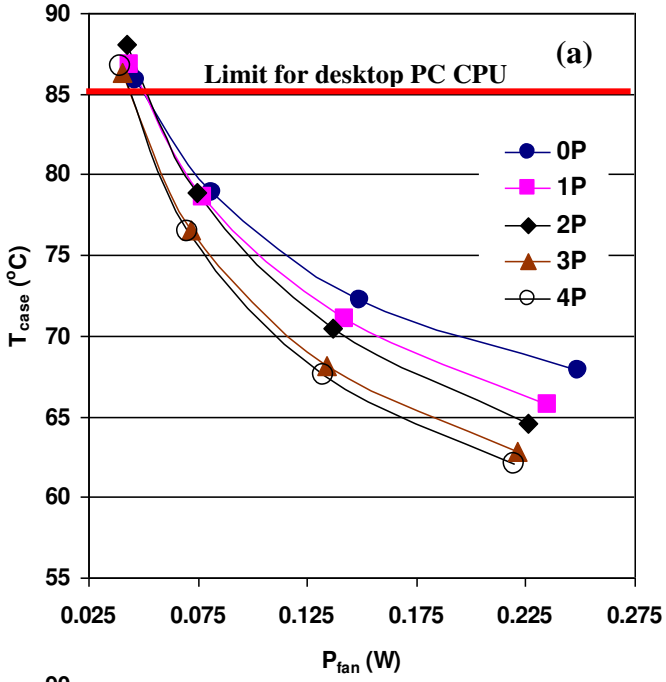
(a)
Limit for desktop PC CPU
0P
1P
2P
3P
4P
90
85
80
75
70
65
60
55
0.025
0.075
0.125
0.175
0.225
0.275
T case (°C)
P fan (W)

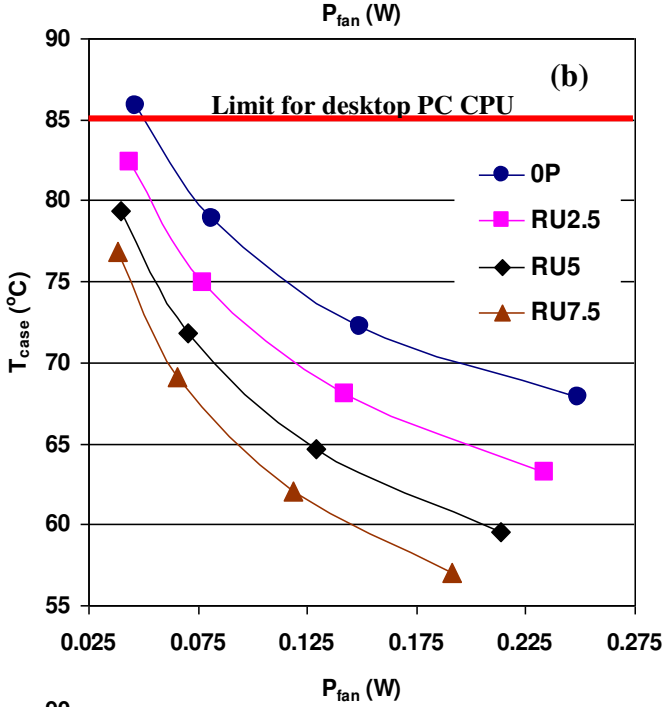
(b)
Limit for desktop PC CPU
0P
RU2.5
RU5
RU7.5
90
85
80
75
70
65
60
55
0.025
0.075
0.125
0.175
0.225
0.275
T case (°C)
P fan (W)

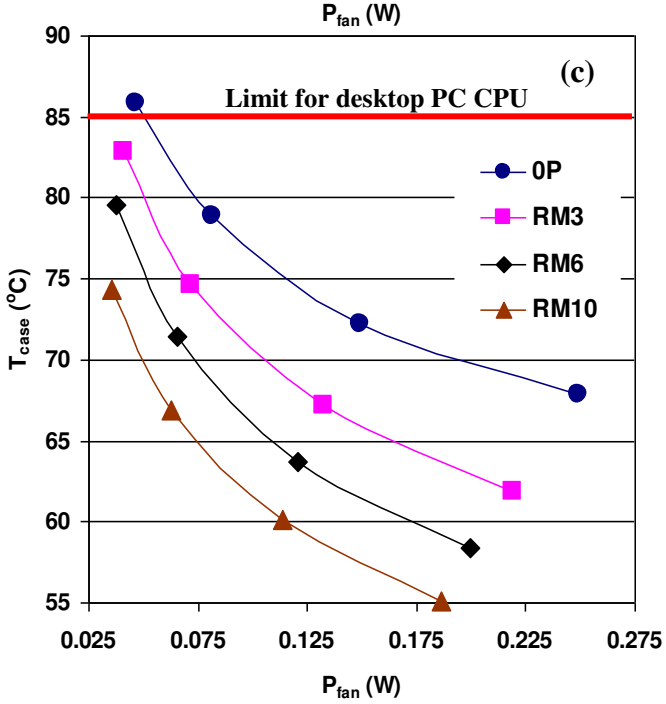
(c)
Limit for desktop PC CPU
0P
RM3
RM6
RM10
90
85
80
75
70
65
60
55
0.025
0.075
0.125
0.175
0.225
0.275
T case (°C)
P fan (W)

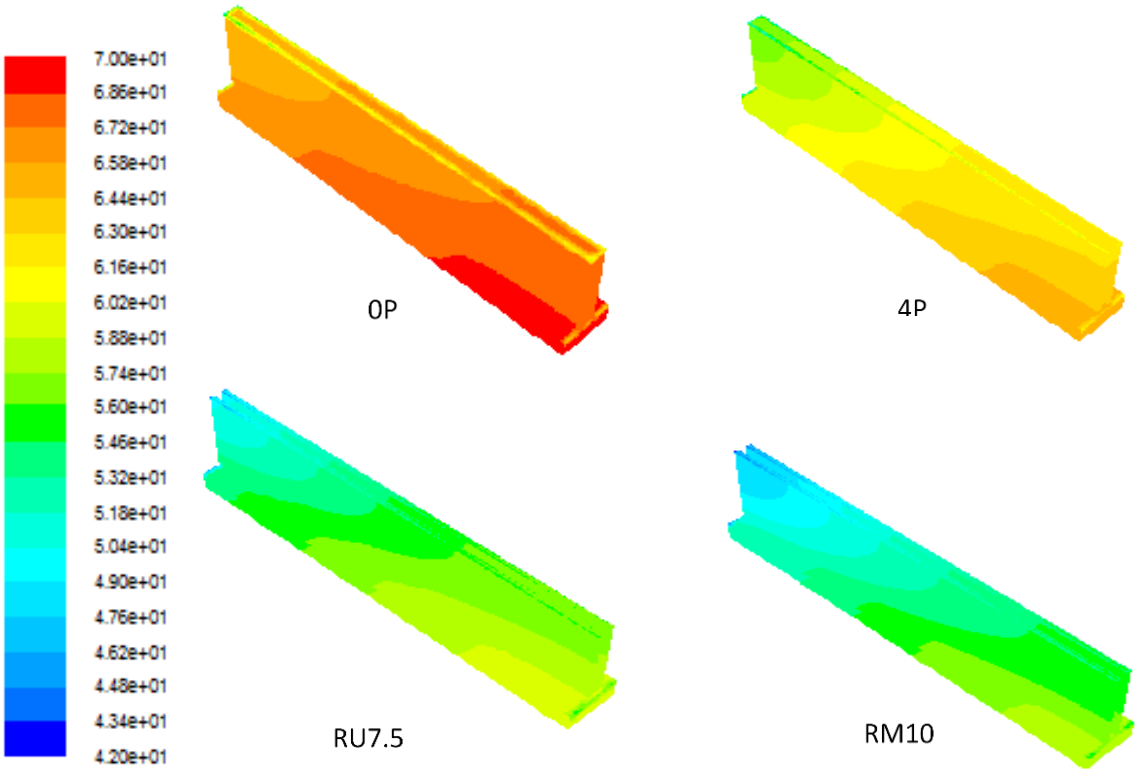

Fig. 8: Temperature distribution on 0P, 4P, RU7.5 and RM10 fins.

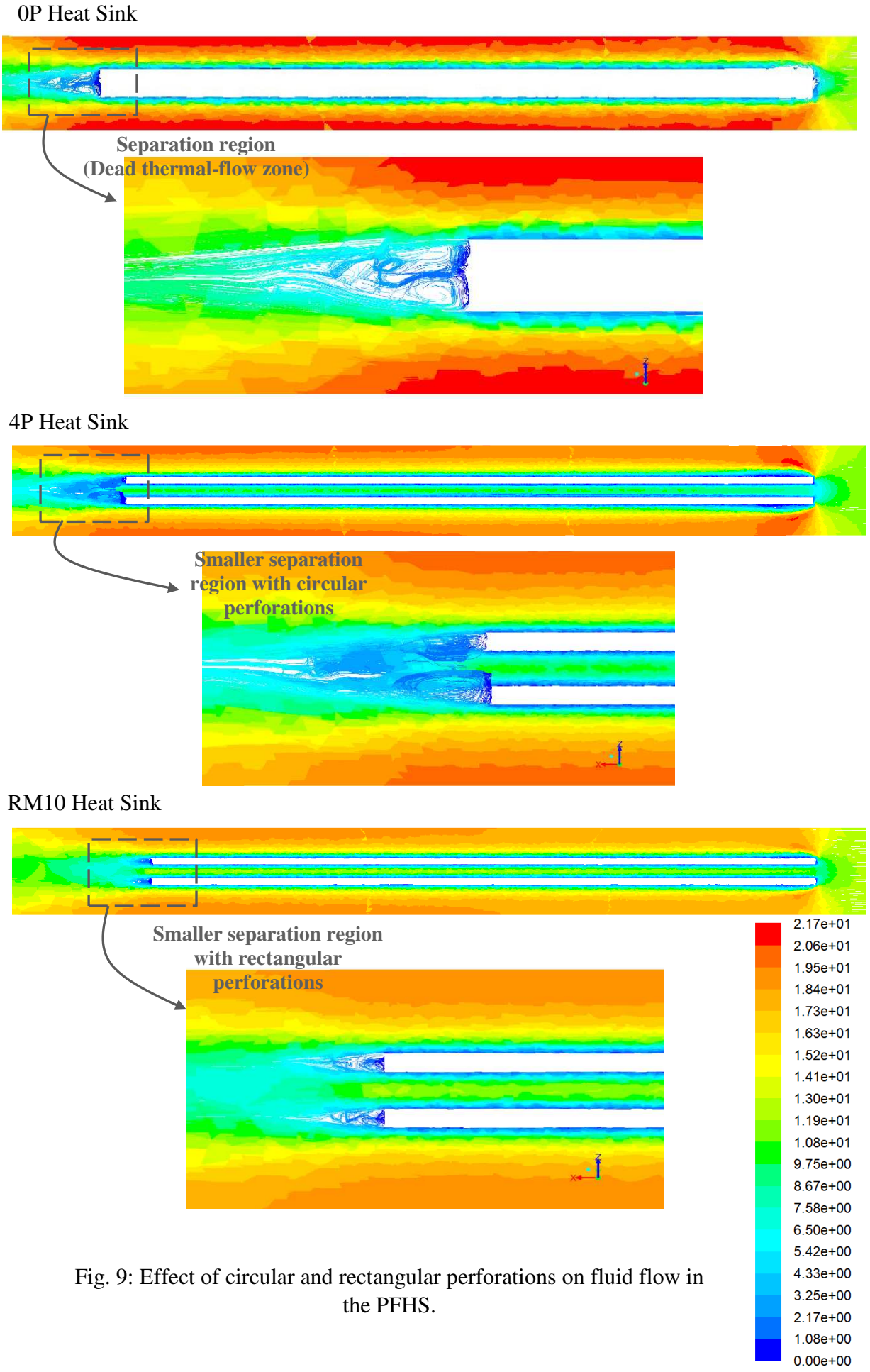

Fig. 9: Effect of circular and rectangular perforations on fluid flow in the PFHS.

Table 1: Effect of grid density for solid PFHS and RM10 PFHS.

Model	Number of Cells	The base temperature (°C)	Pressure drop (Pa)
0P PFHS	11313	88.85	24.2
	36348	87.35	22.0
	103449	85.85	21.0
	229098	85.65	20.8
RM10 PFHS	145902	68.55	17.4
	650000	73.85	16.9
	799835	74.35	16.2
	920000	74.33	16.2

Table 2: Masses of the examined heat sinks.

Model	Mass of solid geometry (g)	Reduction percentage
0P	35.25	0
1P	34.40	2%
2P	33.55	5%
3P	32.70	7%
4P	31.85	10%
RU2.5	32.54	8%
RU5	29.83	15%
RU7.5	27.12	23%
RM3	32.00	9%
RM6	28.74	18%
RM10	24.40	31%

Table 3: Comparison in performance improvements for the modified models in comparison with solid PFHS.

Pin design	% increase in h_p	% reduction in P_{fan}	% reduction in T_{case}
1P	2	5	1
2P	3	9	1
3P	7	12	4
4P	9	13	4
RU2.5	12	5	5
RU5	22	14	10
RU7.5	31	20	13
RM3	12	12	6
RM6	22	19	11
RM10	35	24	16